International Journal of Disaster Risk Reduction 10 (2014) 419–427

Contents lists available at ScienceDirect

International Journal of Disaster Risk Reduction

journal homepage: www.elsevier.com/locate/ijdrr

Probabilistic seismic hazard assessment at global level

Mario G. Ordaz [a], Omar-Darío Cardona [b], Mario A. Salgado-Gálvez [c,*], Gabriel A. Bernal-Granados [c], Shri Krishna Singh [d], Daniela Zuloaga-Romero [e]

[a] Instituto de Ingeniería, Universidad Nacional Autónoma de México (UNAM), México, DF, México
[b] Instituto de Estudios Ambientales (IDEA), Universidad Nacional de Colombia, Sede Manizales, Manizales, Colombia
[c] Centre Internacional de Mètodes Numèrics en Enginyeria (CIMNE), Universitat Politècnica de Catalunya, Edifici C-1, Despatx C-111, Carrer Gran Capita, s/n Campus Nord UPC, 08034 Barcelona, Spain
[d] Instituto de Geofísica, Universidad Nacional Autónoma de México (UNAM), México, DF, México
[e] Illinois Institute of Technology, Chicago, United States of America

ARTICLE INFO

Article history:
Received 29 October 2013
Received in revised form
3 April 2014
Accepted 5 May 2014
Available online 22 May 2014

Keywords:
Global probabilistic seismic hazard analysis
Stochastic scenarios
Smoothed seismicity
Hazard maps

ABSTRACT

In the framework of the UNISDR's Global Assessment Report on Disaster Risk Reduction 2013, for the first time, a fully probabilistic seismic hazard assessment was conducted at global level, using the same methodology for the whole Globe, from which a set of stochastic scenarios for different intensities (spectral accelerations, 5% damping) was obtained and then used in a fully probabilistic risk analysis. First, the Globe was divided into a set of seismogenetic areas to which a maximum magnitude and a predominant tectonic environment type were assigned. A Gutenberg–Richter magnitude–frequency distribution was assumed for each region, with *a* and *b*-values computed using a smoothed-seismicity procedure based on the NEIC[1]-USGS[2] seismic catalog. This catalog was first subjected to a declustering process and completeness verification for several threshold magnitudes. Based on the tectonic environment assigned to each source, a ground motion prediction model was assigned accordingly. Probabilistic hazard computations were performed with program CRISIS 2012, which generated conventional hazard curves for different intensities and maps for various return periods, as well as a set of stochastic scenarios compatible with the CAPRA[3] platform. These scenarios, in turn, were used to perform coarse-grain probabilistic risk computations.

1. Introduction

For the Global Assessment Report on Disaster Risk Reduction 2013 (GAR-13), prepared by the United Nations International Strategy for Disaster Risk Reduction, a coarse-grain probabilistic seismic risk assessment at global level was conducted, using the same methodology and base information for all analyzed zones. The main objective of this analysis was to perform a fully probabilistic risk analysis. However, as a by-product of these computations we also obtained hazard results in terms of exceedance rate curves for different spectral ordinates, uniform hazard

* Corresponding autor. Tel.: +34 603 681 219; fax: +34 934 010 796.
E-mail addresses: mors@pumas.iingen.unam.mx (M.G. Ordaz), odcardonaa@unal.edu.co (O.-D. Cardona), mario.sal.gal@gmail.com (M.A. Salgado-Gálvez), gabernal@cimne.upc.edu (G.A. Bernal-Granados), krishna@ollin.geofisica.unam.mx (S.K. Singh), dzuloaga@hawk.iit.edu (D. Zuloaga-Romero).

[1] National Earthquake Information Center.
[2] United States Geological Survey.
[3] Comprehensive Approach to Probabilistic Risk Assessment.

http://dx.doi.org/10.1016/j.ijdrr.2014.05.004
2212-4209/

spectra and seismic hazard maps for different return periods, as well as a stochastic set of scenarios generated for different spectral accelerations ranging from 0.0 to 2.0 s, for 5% damping, at global level. This paper presents the description and results of this assessment

The analysis started with the most updated available seismic catalog, to which careful completeness analyses and declustering processes were applied. A classical probabilistic seismic hazard analysis (PSHA) was conducted using Gutenberg–Richter (GR) relationships to describe source seismicity, which was given to the calculating code by means of different grids covering the Globe, with a constant spacing in both directions, 720,000 nodes each, and placed at different depths. Completeness verification was conducted for the catalog using the selected threshold magnitude (M_0) of 4.5, after which a seismicity smoothing process was employed to calculate the spatially-varying *a*- and *b*- parameters of the GR relationships of each source. The globe was divided into tectonic regions so that a maximum expected magnitude value (M_U) and a ground motion prediction equation (GMPE) could be assigned to each one of them.

It is worth noting that several very valuable studies had previously assessed the seismic hazard of the Globe based on regional contributions [1,2], where input data, assumptions and calculation methodologies varied from zone to zone. As it had been mentioned before, the results presented in this paper come from a study in which al seismogenetic zones of the World were treated with the same methods.

2. Catalog of events

For the classic PSHA analysis, a catalog of events is required to calculate the seismicity parameters for the various seismogenetic regions. For this case, the NEIC-USGS catalog was employed and complemented with other information sources reported by the same agency.

Using a threshold magnitude (M_0) of 4.5 (M_W) and a completeness analysis following the procedure proposed by Titnti and Mulargia [3], it was found that from 1973 on, the catalog could be considered complete. This can be seen in Fig. 1.

Between January 1973 and January 2012 about 296,274 events were recorded in the original catalog. However,

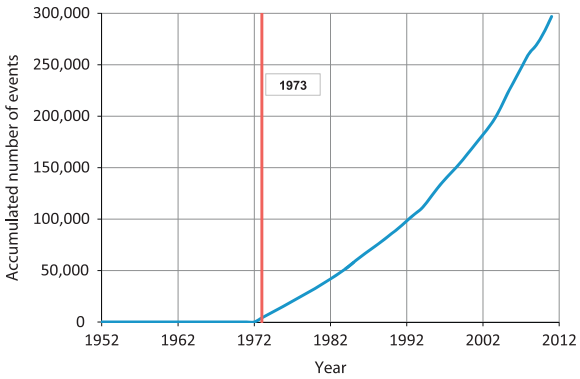

Fig. 1. Completeness verification for M_o=4.5.

since the selected seismicity model assumes that events are independent, a declustering process is conducted, resulting in a total of 151,520 events which are considered for the seismicity parameters calculation. Each of these events has at least the following attributes:

- Date (day, month, year)
- Time (hour, minute, second)
- Longitude
- Latitude
- Depth
- Magnitude

Fig. 2 illustrates the geographical distribution of the considered events, and Table 1 presents some statistics in terms of number of events with magnitude equal or higher than the indicated.

3. Definition of the tectonic regions

Since some of the required seismicity parameters, such as M_U, cannot be calculated through statistical methods, a set of tectonic regions is defined. Most of Earth's seismicity is concentrated along plate boundaries. The hypocentres and focal mechanisms of earthquakes define the location and the nature of the plate interfaces. There is also seismicity in the interior of the plates, away from the plate boundaries including events that occur in the interior of the subduction plates. Of special importance in seismic hazard are the crustal earthquakes in continental plates which often occur far away from the plate boundaries.

For the purpose of seismic hazard estimation, the division of Earth's surface in seismotectonic provinces was based on the knowledge of the plate boundaries, the seismicity and focal mechanisms and geological mapping of active faults using the Global Centroid Moment Tensor (GCMT).[4] The 50 regions defined by Flinn and Engdahl [4], and the NEIC-USGS seismicity catalog are used as base for the definition of the tectonic regions, from which the final tectonic provinces that are presented in Fig. 3 are delimited.

Focal mechanisms of all earthquakes reported in GCMT, considering also the depth of the events, were plotted for each of the Flinn–Engdahl regions; then, maps were carefully analyzed and, based on seismotectonics of the regions, different polygons were traced to delineate the seismotectonic provinces. Based on that information, a depth range was assigned to each province. Earthquakes in each province were assigned to one of the following types in order to assign an appropriate GMPE to compute seismic hazard:

- interplate subduction thrust;
- intraslab in the subducting plate;
- stable continental;
- active crustal (but not plate boundary);
- active crustal (mainly strike-slip, plate boundaries);
- off shore.

[4] http://www.globalcmt.org

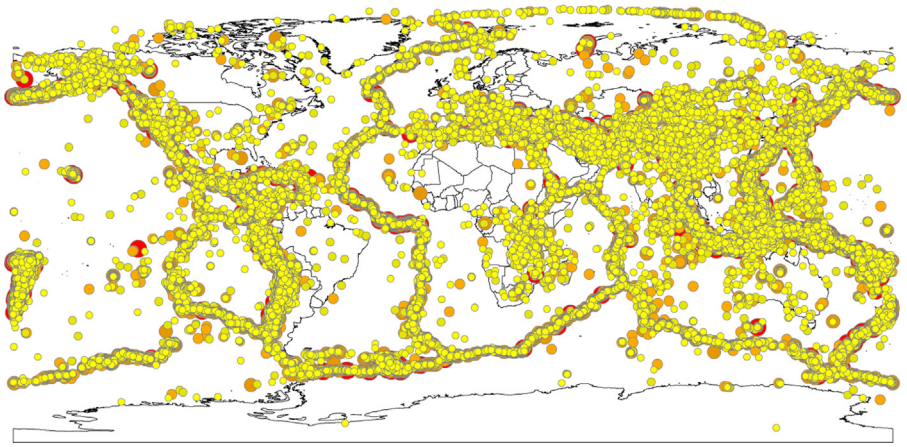

Fig. 2. Epicenters of the events in the catalog.

Table 1
Number of events with magnitude equal or higher than the indicated.

Magnitude	Number of events
4.5	151,520
5	54,057
5.5	15,572
6	4697
6.5	1509
7	488
7.5	166
8	29
8.5	5
9	2
9.1	1

Finally, the compiled data were analyzed for consistency, and borders were adjusted according to the NEIC-USGS catalog. Fig. 3 provides a glance at the seismotectonic provinces. The total number of provinces is 132. Each province has assigned a type or category using the codes that are presented below:

(1) intraplate subduction thrust;
(2) intraslab in the subducting plate;
(3) stable continental;
(4) active crustal;
(5) strike slip;
(6) off shore.

For visualization purposes it is not possible to see the ones classified as (2) though they exist in the model; often the same polygon in different depth range defines different provinces.

4. Seismicity parameters

In view of the global character of the analysis, a smoothed seismicity approach was selected for the calculation of the seismicity parameters. Since earthquakes occur at different depths, three different grids were used, each of them covering the following depth ranges 0–30 km, 30–60 km and more than 60 km. These grids were then located at 15, 45 and 75 km respectively for the seismic hazard analysis. Fig. 4 presents the distribution by number of events in the catalog by depth ranges. It is worth mentioning that in some seismic catalogs such as the one reported by GCTM, a threshold focal depth of 33 km is assigned to earthquakes whose focal depths are difficult to calculate and then this can distort in some way the results and statistics presented below. Though, since seismicity is grouped at the above mentioned depths, the focal depth reporting error can be considered as somehow accounted for since it is not assigned directly to the reported depth but to 45 km.

Each grid was constructed with a spacing equal to 0.3° in both directions, covering the Globe, and for the calculation of the a and b-values (also denoted in this paper as λ_0 and β, respectively) at each node the methodology proposed by Woo [5] was followed. The smoothing radius was defined with the following two parameters:

- $R_{min}=0.3°$;
- $R_{max}=1.2°$.

A weighting process is also required for the definition of these values, as a function of the focal distances of the events to the node on the grid that is being characterized. The weights for the smoothing process are calculated as follows:

- C/R_{min} if $R < R_{min}$;
- C/R if $R_{min} < R < R_{max}$;
- 0 if $R > R_{max}$

where R is the focal distance between the event in the seismic catalog and the node on the grid that is being characterized. In addition, in order to avoid errors due to small samples, the values of β were truncated between 1.8 and 3.0 for each node in the smoothed grid.

Fig. 5 presents the smoothed seismicity grid for the λ_0 parameter while Fig. 6 presents the smoothed seismicity

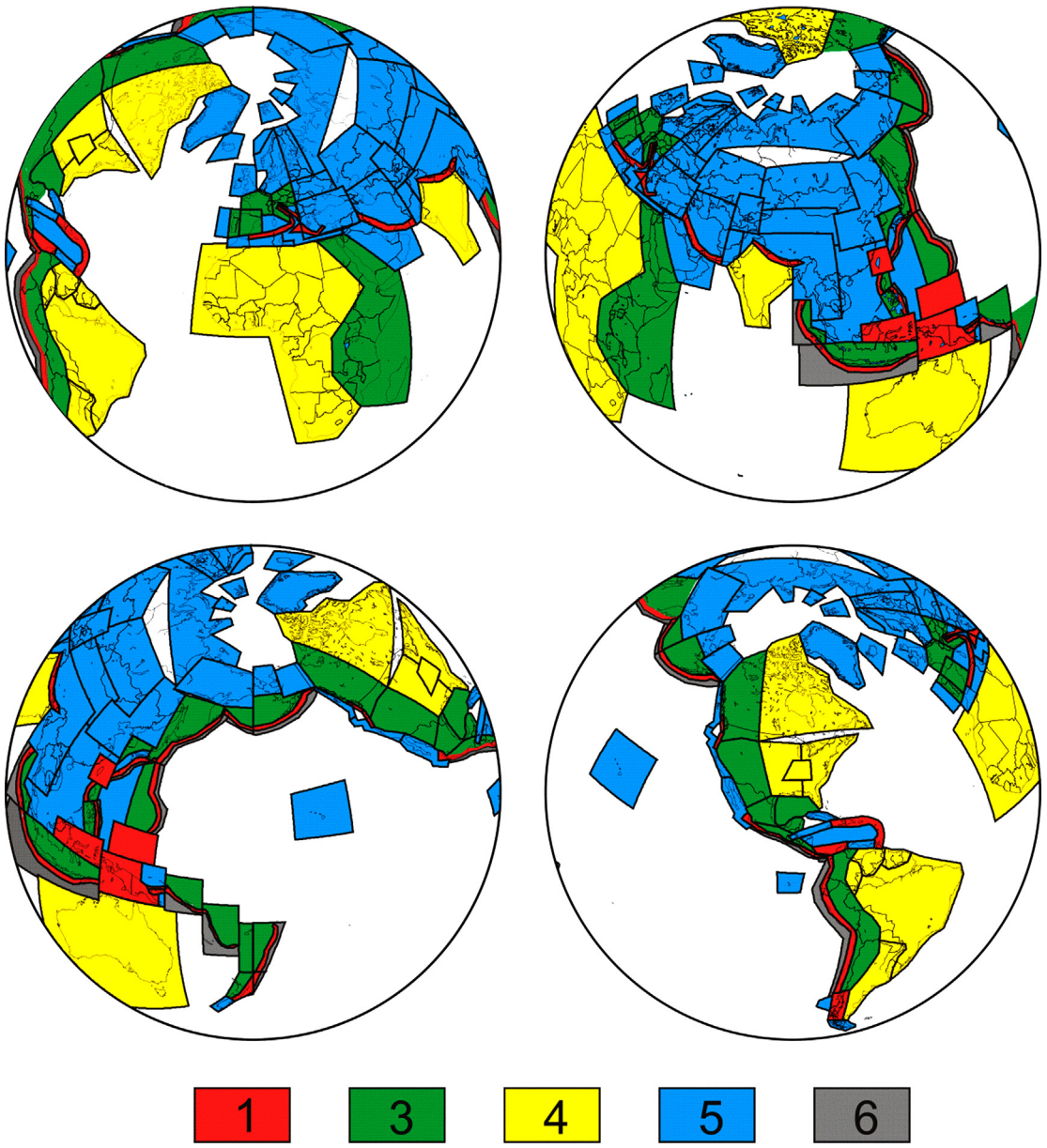

Fig. 3. Tectonic regions defined for the analysis.

grid for the β parameter. Both grids correspond to the first depth range mentioned above.

5. Selected seismicity model

For the analysis, a modified version of the Gutenberg–Richter relationship was selected as a seismicity model for all seismogenetic sources; the activity of the *i*th seismic source, in this case a node in any of the defined grids, is specified in terms of the magnitude exceedance rates, $\lambda_i(M)$, generated by each node. The magnitude exceedance rate defines how frequently earthquakes of different magnitudes are generated in each of the sources. In this case, the seismicity is represented by the following equation [6]:

$$\lambda(M) = \lambda_0 \frac{e^{-\beta M} - e^{-\beta M_U}}{e^{-\beta M_0} - e^{-\beta M_U}} \quad (1)$$

where M_0 is the threshold magnitude, and λ_0, β_i, and M_U are parameters that define the exceedance rate for each source, as shown in Fig. 7.

Parameter λ_0 is the average annual number of events in each node with magnitude equal or higher than the threshold, β represents the slope of the initial part of the logarithmic regression, and M_U is the maximum expected magnitude at each node. The latter parameter is defined considering the tectonic environment, as explained in the previous section. As a result of this, each node on the different grids is characterized with three seismicity

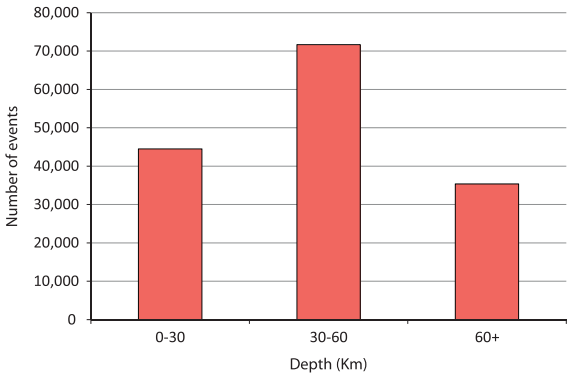

Fig. 4. Number of events in the catalog associated with the selected depth ranges.

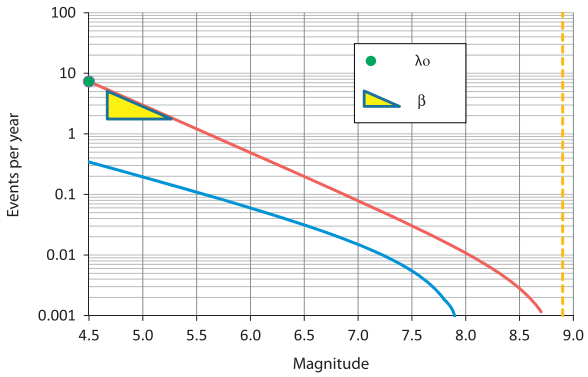

Fig. 7. Examples of the magnitude exceedance rates used in this paper. (For interpretation of the references to color in this figure, the reader is referred to the web version of this article.)

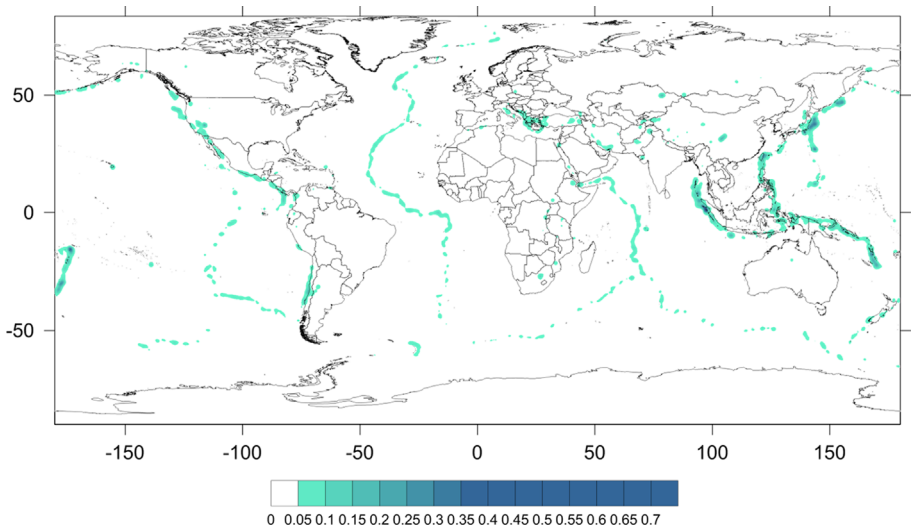

Fig. 5. λ_o (1/year) grid for the 0–30 km depth range.

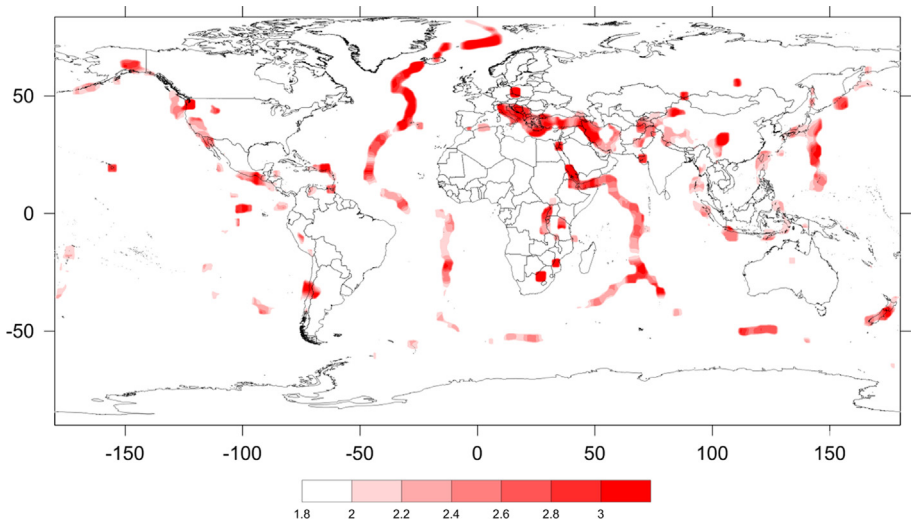

Fig. 6. β grid for the 0–30 km depth range.

parameters. Fig. 7 shows an example where the blue and red lines represent two hypothetical sources' magnitude exceedance rates and the dashed vertical yellow line the maximum magnitude, M_U assumed equal for both of them.

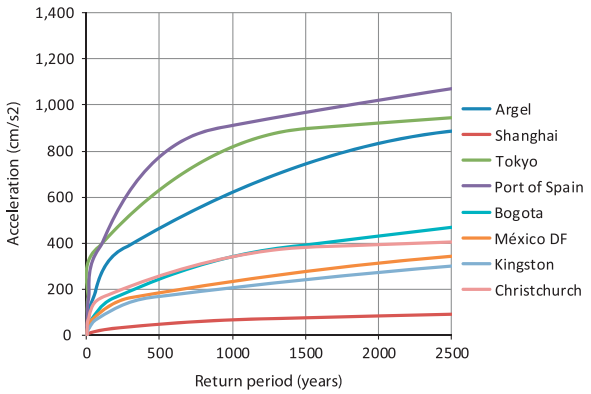

Fig. 8. PGA seismic hazard curves for different cities.

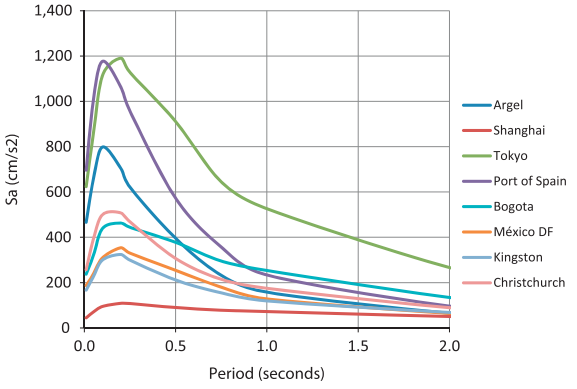

Fig. 9. Uniform hazard spectra for different cities and 475 years return period.

From the figure it is evident that the source associated to the red line has higher seismic activity.

6. Ground motion prediction equations

Keeping in mind the global scope of the analysis, a revision of proposed GMPEs for different tectonic environments was conducted. The GMPEs used for this analysis were the five GMPEs proposed in the framework of the GEM1 Project, associated to the Global Earthquake Model (GEM) Initiative, as follows:

- Abrahamson and Silva [7] (active crustal, plate boundary);
- Atkinson and Boore [8] (stable continental);
- Cauzzi and Faccioli [9] (active crustal, not plate boundary, and offshore);
- Youngs Interface [10] (interplate subduction thrust);
- Youngs Intraslab [10] (intraslab in the subducting plate).

As was mentioned above, only one GMPE was assigned to each type of tectonic region.

7. Seismic hazard assessment

Program CRISIS 2012 [11] was used for the hazard calculations, given its ample capabilities as well as its compatibility with the CAPRA platform. Once the seismicity parameters and the GMPEs are known for each node in all three grids, the seismic hazard can be calculated considering the effects of the totality of the nodes and their corresponding distances to the site of interest. Finally, the seismic hazard expressed in terms of intensity exceedance rates, $\nu(a)$, is calculated with the following expression:

$$\nu(a) = \sum_{n=1}^{N} \int_{M_0}^{M_U} -\frac{\partial \lambda}{\partial M} \Pr(A > a | M, R_i) dM \qquad (2)$$

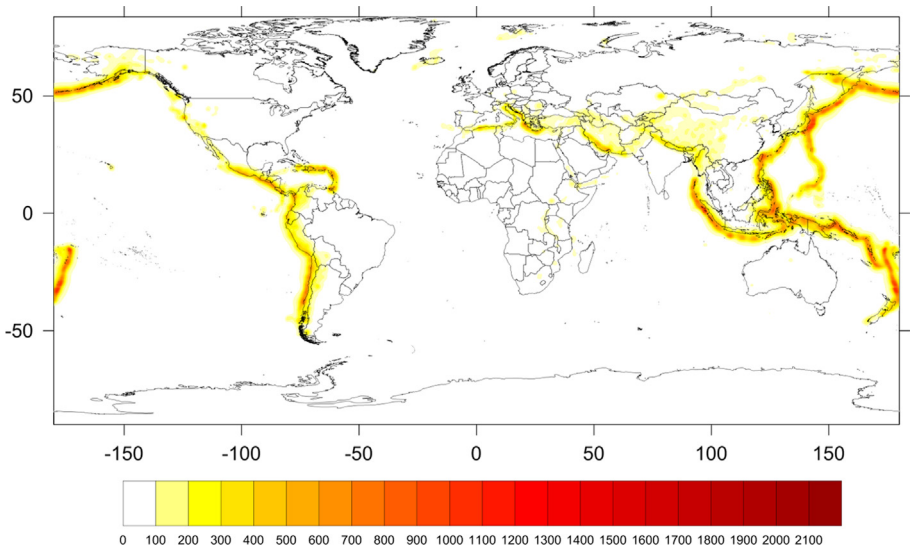

Fig. 10. PGA (cm/s^2) seismic hazard map. Return period 225 years.

where the sum covers the totality of the nodes, N, located within the integration distance, set in this case equal to 300 km, and $\Pr(A > a|M,R_i)$ is the probability that the intensity exceeds a certain value given the magnitude of the earthquake M, and the distance between the ith source and the analysis point R_i. The $\lambda_i(M)$ functions are the earthquake magnitude exceedance rates. The integration is carried out between M_0 and M_U, which indicates that, for each node, the contribution of all possible magnitudes is considered.

Assuming that given the magnitude and the distance, the intensity follows a lognormal distribution, the probability $\Pr(A > a|M,R_i)$ is calculated as follows:

$$\Pr(A > a|M,R_i) = \Phi\left(\frac{1}{\sigma_{Lna}} \ln \frac{MED(A|M,R_i)}{a}\right) \quad (3)$$

where $\Phi(\ )$ is the normal standard distribution, $\mathrm{MED}(A|M, R_i)$ is the median of the intensity, given by the associated GMPE for known magnitude and distance, and σ_{Lna} denotes the standard deviation of the natural logarithm of the intensity.

8. Seismic hazard assessment results

This section presents a summary of the obtained results in terms of exceedance curves for peak ground acceleration (PGA), shown in Fig. 8, uniform hazard spectra for 475 years return period for selected cities, shown in Fig. 9, and a set of seismic hazard maps for different spectral ordinates and return periods (all for 5% damping), shown in Figs. 10–15.

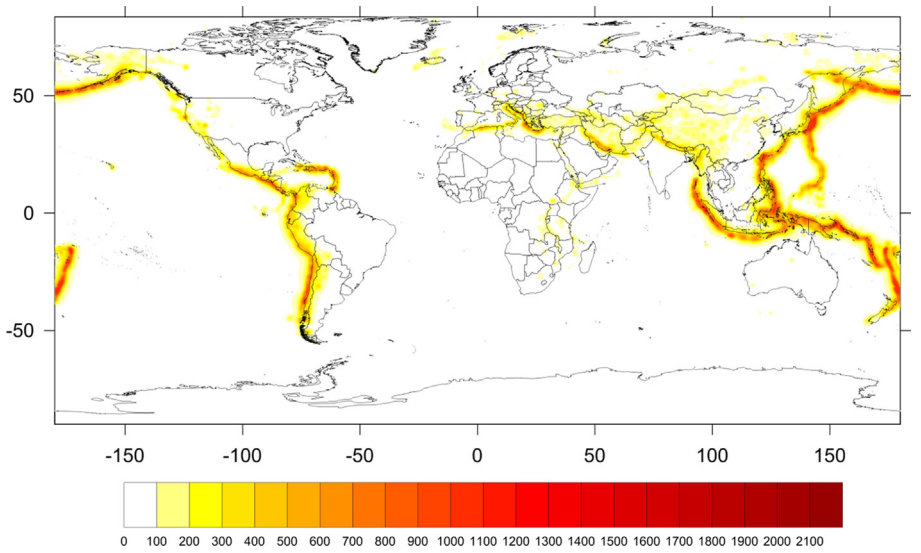

Fig. 11. PGA (cm/s^2) seismic hazard map. Return period 475 years.

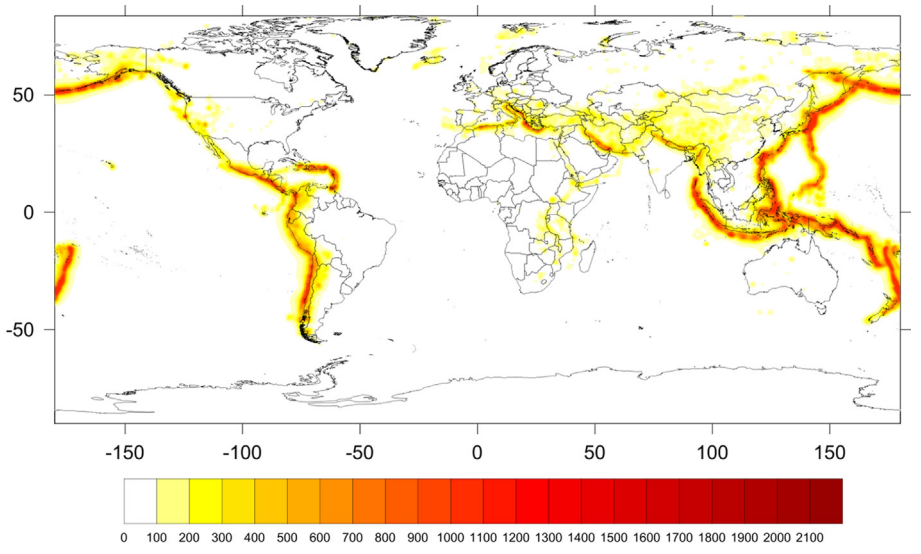

Fig. 12. PGA (cm/s^2) seismic hazard map. Return period 1000 years.

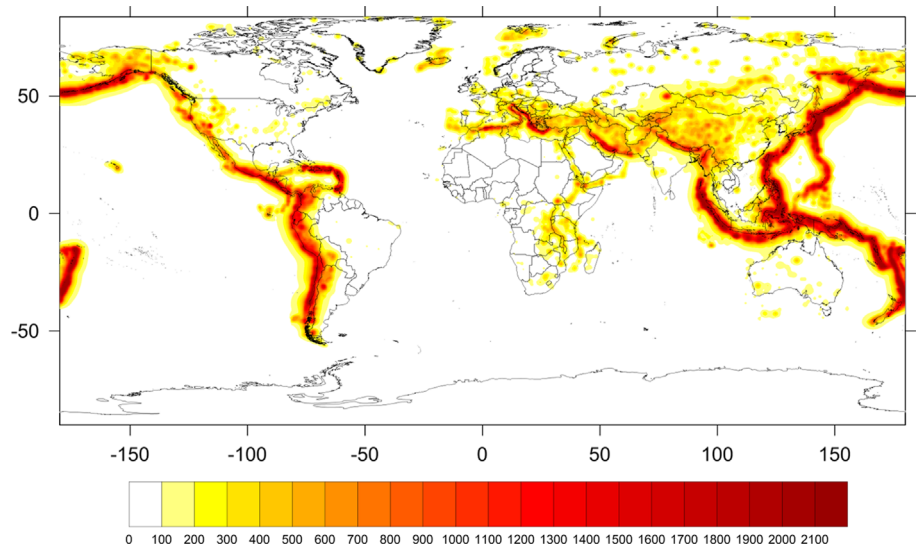

Fig. 13. Seismic hazard map for the spectral acceleration (cm/s^2) at $T=0.2$ s. Return period 2500 years.

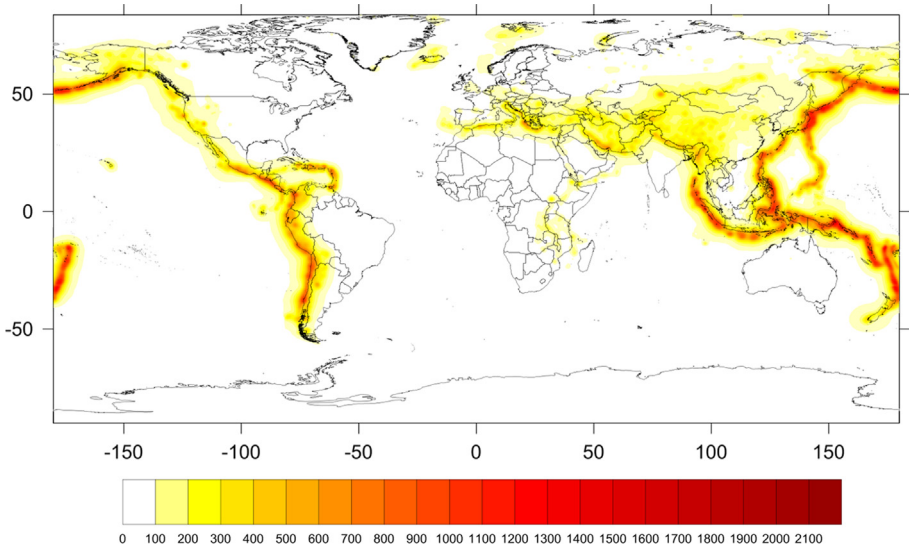

Fig. 14. Seismic hazard map for the spectral acceleration (cm/s^2) at $T=0.5$ s. Return period 475 years.

Hazard maps are obtained by using the intensity exceedance rate plots at each node of the calculation grids, and then it is evident that for obtaining the above shown maps a large set of hazard curves are obtained, one for each node and for each spectral ordinate, as a seismic hazard calculation output. Also, it is well know that when the intensity exceedance rates are known at a point of interest and the exposed assets are characterized with a vulnerability function, physical risk can be computed in terms of the average annual loss (AAL). Even though it represents the most robust way to quantify risk and allows comparing the results, this metric does not present the complete risk panorama for the exposed assets. When calculating risk using a scenario approach, it is possible to obtain for the analyzed portfolios, their loss exceedance curve (LEC) that relates the expected losses, usually expressed in monetary terms, with their frequency of exceedance. For this case, a stochastic set of earthquakes, comprised by 1,022,129 scenarios, was generated, each of them containing expected intensities and their standard deviations for 23 spectral ordinates between 0.0 and 2.0 s.

Since each scenario has an associated frequency of occurrence of an intensity field, the portfolio AAL can be directly computed from the stochastic set as a sum of the expected losses for each asset weighted by the frequency of occurrence associated with each scenario. More important, the stochastic event set allows computation of the full LEC, from where the losses associated to several return periods can be derived.

9. Conclusions

For the first time, a probabilistic hazard assessment has been conducted at global level using the same seismic

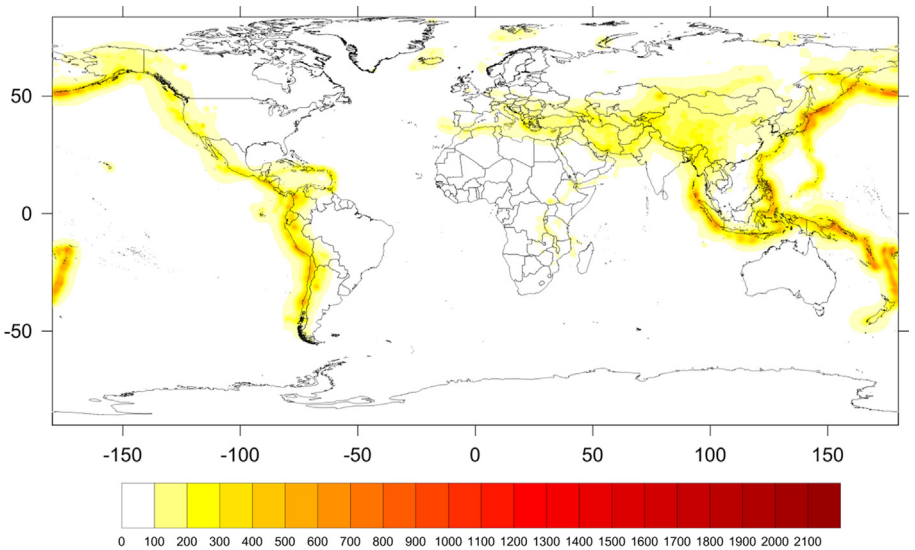

Fig. 15. Seismic hazard map for the spectral acceleration (cm/s^2) at $T=1$ s. Return period 475 years.

catalog and methodology for the definition of tectonic regions. In addition, a globally consistent methodology was used to compute the seismic hazard. Because of the global and coarse-grain scope of the analysis, it was considered inconvenient to define a large set of faults or areal seismogenetic sources, and instead, a smoothed seismicity approach was chosen for the calculation of the seismicity parameters.

Because spectral GMPEs were selected and used, seismic hazard results were obtained in terms of intensity exceedance rates for different spectral ordinates, and based on this, uniform hazard spectra were derived. In addition to this classical representation of the seismic hazard results, a stochastic set of earthquakes comprised by more than a million scenarios, each of them with 23 associated intensities was generated for the Globe for the first time.

The set of stochastic earthquake scenarios was then used in the Global Risk Assessment (GRA) [12] to compute, in a fully probabilistic way, seismic risk at country level, where AAL were obtained for more than 200 countries, PML for a fixed return period of 250 years and the complete LEC curve for a set of countries.

References

[1] Giardini D, Grüntal G, Shedlock K, Zhang P. The GSHAP global seismic hazard map. Ann Geofis 1999;42(6):1225–30.

[2] Muir-Wood R. From global seismotectonics to global seismic hazard. Ann Geofis 1993;36(3–4):153–68.

[3] Tinti S, Mulargia F. An improved method for the analysis of the completeness of a seismic catalogue. Lett Al Nuovo Cimento Ser 2 1985;42(1):21–7.

[4] Flinn EA, Engdahl ER. A proposed basis for geographical and seismic regionalization. Rev Geophys 1965;3:123–49.

[5] Woo G. Kernel estimation methods for seismic hazard area source modeling. Bull Seismol Soc Am 1996;68(2):353–62.

[6] Cornell, CA, and Van Marke EH. The major influences on seismic risk. In: Proceedings of the third world conference on earthquake engineering, Santiago, Chile, A-1; 1969. p. 69–93.

[7] Abrahamson NA, Silva WJ. Empirical response spectral attenuation relations for shallow crustal earthquakes. Seismol Res Lett 1997;68(1):94–127.

[8] Atkinson G, Boore D. Earthquake ground-motion prediction equations for Eastern North America. Bull Seismol Soc Am 2006;96(6):2181–205.

[9] Cauzzi C, Faccioli E. Broadband (0.05 to 20 s) prediction of displacement response spectra based on worldwide digital records. J Seismol 2008;12:453–75.

[10] Youngs RR, Chiou SJ, Silva WJ, Humphrey JR. Strong ground motion attenuation relationships for subduction zone earthquakes. Seismol Res Lett 1997;68(1):58–73.

[11] Ordaz M, Martinelli F, Aguilar A, Arboleda J, Meletti C, D'Amico V. CRISIS 2012, program for computing seismic hazard. Instituto de Ingeniería, Universidad Nacional Autónoma de México; 2012.

[12] Cardona OD, Ordaz M, Mora MG, Salgado-Gálvez MA, Bernal GA, Zuloaga D, Marulanda MC, Yamin L, González D. Global risk model: a fully probabilistic seismic and tropical cyclone wind risk assessment. In: Probabilistic assessment of risk from natural hazards at global scale, Special Issue of the International Journal of Disaster Risk Reduction.